International Journal of GEOMATE, Nov., 2019 Vol.17, Issue 63, pp. 172 - 180
ISSN: 2186-2982 (P), 2186-2990 (O), Japan, DOI: https://doi.org/10.21660/2019.63.47145
Geotechnique, Construction Materials and Environment

DRAINED SHEAR STRENGTH OF COMPACTED KHON KAEN LOESS FROM MULTISTAGE TRIAXIAL TEST

S. Chatchawan [1] and *R. Nuntasarn[2]

[1,2,] Faculty of Engineering, Khon Kaen University, Thailand

* Corresponding Author, Received: 11 Feb. 2019, Revised: 15 April 2019, Accepted: 05 May 2019

ABSTRACT: The previous research found that Khon Kaen loess is collapsible soil. The structure of Khon Kaen loess is a honeycomb structure and loose adhesion. The cause of losing shear strength and collapsing is the increase in moisture content. The purpose of this study was to investigate the influence of matric suction on the shear strength of compacted Khon Kaen loess by a multistage consolidated drained triaxial test. According to the soil water characteristic curve, the matric suction of this study consists of saturation regime at matric suction of 0 kPa, transition regime at matric suction of 10 kPa, and the residual regime at matric suction of 50 kPa and 100 kPa. The testing result indicated that the cohesion intercept (c) is non-linearly increasing with matric suction. The effective friction angle (ϕ') is also increasing with matric suction. However, the angle with respect to changes in matric suction (ϕ^b) is gradually decreasing. According to the test result, the active earth force (P_a) decreases with increasing matric suction. However, the bearing capacity was increased with increasing matric suction. Therefore, the matric suction influences the size of the cantilever wall. In conclusion, this research shows that matric suction influences the shear strength of Khon Kaen loess. Furthermore, the unsaturated shear strength is useful and alternative to foundation design because the width of the foundation is not excessive, saving material costs.

Keywords: Triaxial Test, Unsaturated, Consolidated Drained, Compacted Khon Kaen Loess, Matric Suction

1. INTRODUCTION

Khon Kaen loess in Thailand is classified as collapsible soil. The structure of Khon Kaen is honeycomb, which is a metastructure. When moisture increases, causes the loss of shear strength of the soil and collapses suddenly. Udomchoke [1] found that the shear strength parameters of Khon Kaen loess are decreased with increases in the moisture content, as shown in Fig. 1 and 2. Moreover, [1] also found that the collapsing index of Khon Kaen loess illustrated the severe degree of collapsing. Therefore, Khon Kaen loess is called collapsible soil. Therefore, the shear strength testing of Khon Kaen loess was significant.

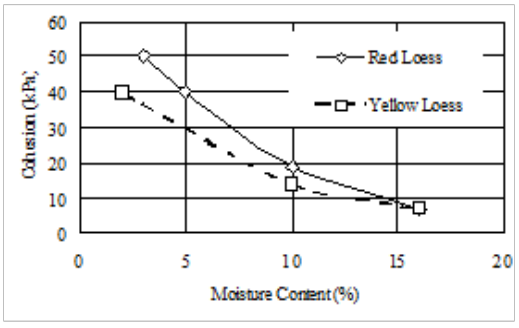

Fig. 1 Variation of the cohesion of Khon Kaen loess with moisture content (Ref [1])

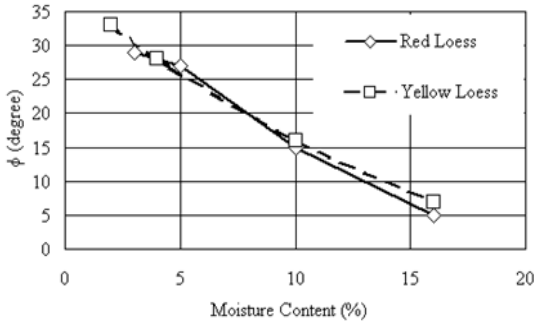

Fig. 2 Variation of the friction angle of Khon Kaen loess with moisture content (Ref [1])

Khon Kaen Province stands 100 to 200 m above mean sea level on a high plateau, which is called the Khorat plateau. Khon Kaen loess is a windblown deposit that is classified as SM, SC, or SM-SC [2]. Khon Kaen loess is found in the first layer of Khon Kaen soil. The thickness of Khon Kaen loess is approximately 2 to 10 m [3]. Moreover, the groundwater table is at great depth. Therefore, Khon Kaen loess often experiences an unsaturated condition rather than a saturated condition.

Gasaluck [4] found that Khon Kaen loess in its natural state has a high coefficient of permeability (k) even after being compacted at 100% by modified compaction.

Hormdee et al. [5] studied the shear strength of Khon Kaen loess by direct shear testing and found

that the shear strength parameter for the multistage method is similar to the single stage method. They concluded that Khon Kaen loess can be tested by a multistage method as shown in Fig. 3. Moreover, [6] also compared the shear strength parameters of Khon Kaen loess in a saturated condition between the single stage and the multistate stage. The result presented a slight difference between c' and ϕ'. Moreover, the multistate method is more rapid and straightforward than the single stage method. Therefore, this study used the multimethod to investigate the drained shear strength parameters.

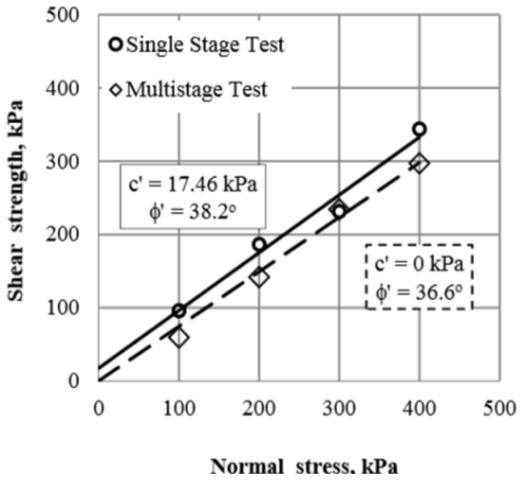

Fig. 3 Failure Envelope in Direct Shear Test (Ref [5])

Khon Kaen loess is experienced at unsaturated conditions rather than saturation conditions. Therefore, the shear strength of Khon Kaen loess cannot be studied by an ordinary equation of [7], because this theory is based on saturated soil. [8] proposed a linear shear strength equation for unsaturated soil as shown in Eq. (3).

Moreover, [9] studied the unsaturated shear strength parameters by predicted the matric suction of specimen from SWCC. The test results showed the non-linear relationship between the matric suction and shear strength. After that, [10] presented a conceptual relationship between soil water characteristic curve and unsaturated shear strength envelope as shown in Fig. 4. [11] found that at saturation regime, (ϕ′) and (ϕ^b) were similar. Then matric suction increased with net confining pressure rising at the transition regime. While the saturation regime is changing to the transition regime, (ϕ^b) becomes gradually less than (ϕ′).

Rahardjo [12] studied a consolidated drained test on a residual soil, which was classified as CL according to [2]. This study found that the matric suction influences the shear strength of the soil. At the same confining pressure, a soil with a high matric suction has a higher value of shear strength parameters than soil with low matric suction. The results showed the effective friction angle of 31.5 degrees and a ϕ^b of 29 degrees before air entry value. After air entry value, the relationship between cohesion intercept (c) and matric suction was non-linear, as shown in Fig. 5.

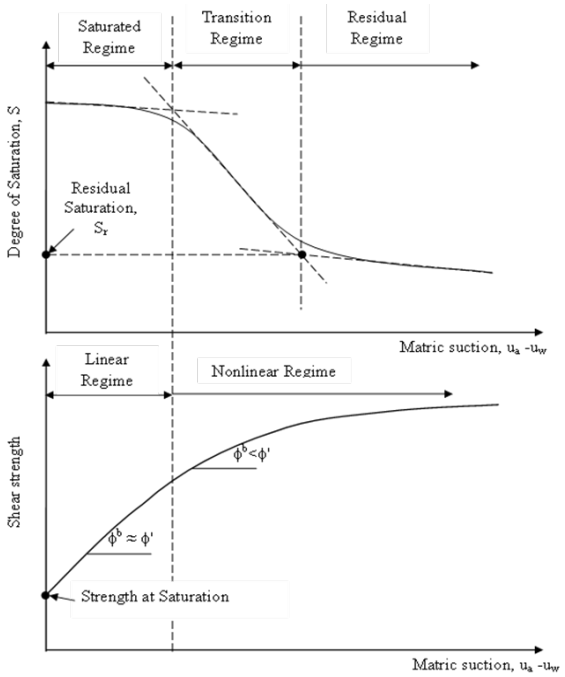

Fig. 4 The Relationship between SWCC and shear strength of unsaturated soil **(**Ref [10])

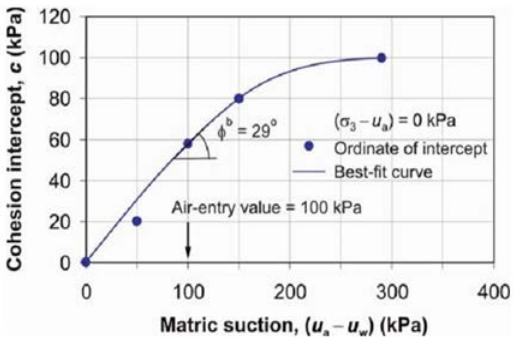

Fig. 5 The relationship between cohesion intercept and matric suction (Ref [12])

Al Aqtash and Bandini [13] studied the unsaturated shear strength of the adobe soil by an unconsolidated undrained direct shear test using the soil-water characteristic curve. The result illustrated that the predicted failure envelopes in the shear strength and matric suction plane were nonlinear, as shown in Fig. 6. The slope of a graph between ϕ^b and matric suction, ϕ^b at saturated state (matric suction equal to zero) was similar to the ϕ′. Then the ϕ^b- value was gradually decreasing with increasing

matric suction until reaching the air-entry (soil reaching transition state). Under the transition regime, the ϕ^b- value was dramatically reduced on increasing the matric suction, as shown in Fig. 7.

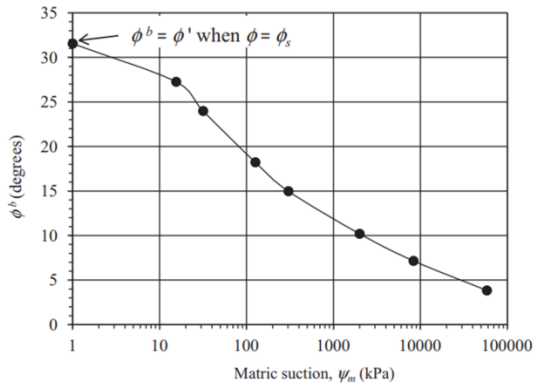

Fig. 6 The relationship between ϕ^b and matric suction (Ref [13])

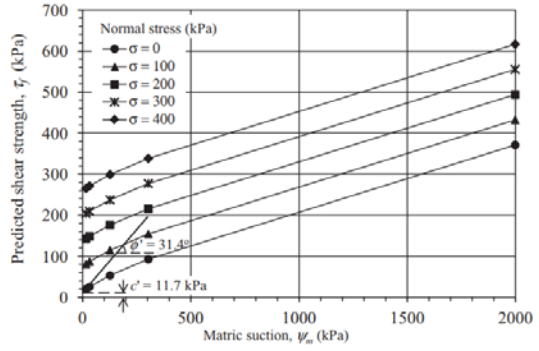

Fig. 7 The relationship between predicted shear strength and matric suction (Ref [13])

2. METHODOLOGY

This study of Khon Kaen loess was undertaken to determine the drained shear strength from the consolidation drained test by a multistage method. Moreover, the soil water characteristic curve (SWCC) was determined from the pressure plate and the isopiestic humidity method. All samples were prepared to achieve 90% wet side of maximum dry density by modified compaction.

2.1 Consolidated drained triaxial test by multistage

The size of the soil specimen for the consolidation drained triaxial test is 50 mm in diameter and 100 mm in height. The specimen was statically compacted to achieve 90% wet side of maximum dry density by modified compaction.

In this study, one specimen was applied one matric suction-value but was subjected to three confining pressures (150, 300, and 600 kPa). According to the SWCC, four values of matric suction were investigated. The first specimen was tested at the saturation state, which is matric suction equal to 0 kPa. The second specimen was screened at the transition regime, with the matric suction value of 10 kPa. The third and the fourth specimens were tested at the residual regime, with the matric suction values of 50 kPa and 100 kPa, respectively, as present in Table 1.

Table 1 Program of this study.

Sample No.	stage	σ_{net} (kPa)	u_a (kPa)	u_w (kPa)	ψ (kPa)
1	1	150	0	20	0
	2	300			
	3	600			
2	1	150	30	20	10
	2	300			
	3	600			
3	1	150	70	20	50
	2	300			
	3	600			
4	1	150	120	20	100
	2	300			
	3	600			

The methodology to determine the unsaturated shear strength parameters by the consolidated drained triaxial test from the multistage method can be divided into three steps according to [14].

Step 1: Saturation. The specimen was compacted, then a soil specimen was set up into a triaxial compression apparatus. After that, apply water pressure into specimen until soil specimen saturated with a B value of 95% by an equation for B value shown in Eq. (1).

$$B = \frac{\Delta u}{\Delta \sigma_3} \quad (1)$$

Where;

Δu = pore pressure change in the chamber pressure when drainage valves closed

$\Delta\sigma_3$ = isotropic change in the chamber Pressure

Step 2: Consolidation. The specimen was consolidated by increasing to the desired net confining pressure following Table 1. Pore air and

pore water pressure were applied to the specimens according to Table 1. Open the drainage valve to drain air and water from the sample. The drainage valve was closed when the sample reached an equilibrium condition. t_{90} was determined from the relationship between square root time and the deformation of the soil sample at this step. Then the rate of shear was calculated from Eq. (2).

$$\varepsilon = \frac{4\%}{16t_{90}} \quad (2)$$

Where;

t_{90} = square root time derived from x- intercept in the relationship of the graph between total volume change and square root time

Step 3: Shearing. The specimen was sheared with the rate that was determined from Eq. (2). Then the shearing was stopped when the specimen almost reached the maximum point of the stress-strain curve. Later, the load was released to 0 kPa.

Step 2 and 3.were repeated. After the final stage, which is stage 3 (σ_{net} = 600 kPa), the specimen was sheared to failure.

This process was repeated with all the specimens. Once the information has been completed, the test results were plotted in 3D to form the extended Mohr-Coulomb failure envelope. The extended Mohr-Coulomb failure envelope consists of shear stress at failure (τ_f), the net stress ($\sigma - u_a$) and matric suction ($u_a - u_w$). The equation of unsaturated soil was proposed by [6], as shown in Eq. (3) and Fig. 8.

$$\tau_f = c' + (\sigma - u_a)_f \tan\phi' + (u_a - u_w)_f \tan\phi^b \quad (3)$$

Where;

τ_f = shear stress at failure

c' = effective apparent cohesion

u_w = pore water pressure

u_a = pore air pressure

$(u_a - u_w)_f$ = matric suction at failure

$(\sigma - u_a)_f$ = the net stress at failure

ϕ' = friction angle of effective stress

σ = total normal stress

ϕ^b = angle indicating the rate of increase in shear strength relative to the soil suction at failure plane

$$c = c' + (u_a - u_w) \tan\phi^b \quad (4)$$

Where;

c = the cohesion intercepted

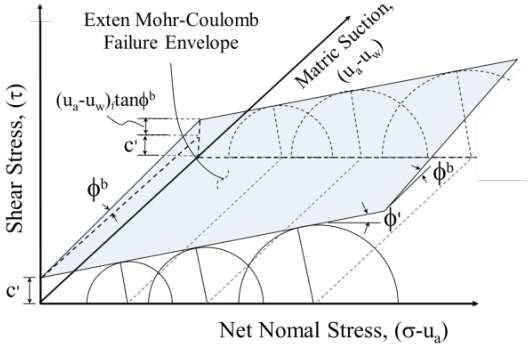

Fig. 8 Extended Mohr-Coulomb failure envelope for unsaturated soil. (Ref [8])

2.2 Soil water characteristic curve

Two methods determined the drying soil water characteristics curve (SWCC). According to [15], the pressure plate method was used to establish SWCC for suction values between 1 to 1,500 kPa. Moreover, SWCC at suctions above 1,500 kPa were determined from the isopiestic humidity method. In this method, three solutions, which were copper sulfate ($CuSO_4$), Ammonium Chloride (NH_4Cl) and sodium hydroxide ($NaOH.H_2O$), were used to determine SWCC at suction values of 3,900 kPa, 30,900 kPa, and 365,183 kPa, respectively. Data points above 1,500 kPa were total suction values [16].

3. RESULTS AND DISCUSSION

The results were separated into three parts. The first part includes the basic properties of Khon Kaen loess. The second part includes the soil water characteristic curve. The third part includes the drained shear strength parameters.

3.1 Basic properties

The sample was collected as a disturbed sample at a depth of 2 m. The index properties and compaction characteristics are shown in Table 2. According to [2], Khon Kaen loess is classified as silty sand (SM). The majority of Khon Kaen loess is sand with a small number of clay particles. The clay particles might play a role as the cementation agent between the sand particles.

The modified compaction test showed that the maximum dry density is 2.12 t/m^3 and that the optimum moisture content is 7.22%. Therefore, the initial dry density and moisture content of the specimen was 1.9 t/m^3 and 11.85%, respectively.

Table 2 Properties of Khon Kaen loess

Properties	
Liquid limit (LL), %	16.5
Plastic limit (PL), %	NP
Plasticity index (PI), %	-
Specific gravity	2.65
Optimum moisture content (OMC), %	7.22
Maximum dry density (ρ_d), t/m^3	2.12
Sand (%)	55
Silt (%)	30
Clay (%)	15
USCS classification	SM

3.2 Soil water characteristic curve

The test result of a pressure plate and isopiestic humidity showed the soil water characteristic curve (SWCC) illustrated in Fig 9. The SWCC of compacted Khon Kaen loess shows a bimodal curve, which indicates two distinct air-entry values and two distinct residual points [17]. This means that there are two pore sizes of compacted Khon Kaen loess. The first and second air entry values are 3 and 450 kPa, respectively. Moreover, the first and second residual degrees of saturation is 42% and 16%, respectively. Therefore, the soil suction values of the saturation regime and the first transition regime were between 0 to 3 kPa and 3 to 27 kPa, respectively. The soil suction, which was higher than 27 kPa, was the first residual regime.

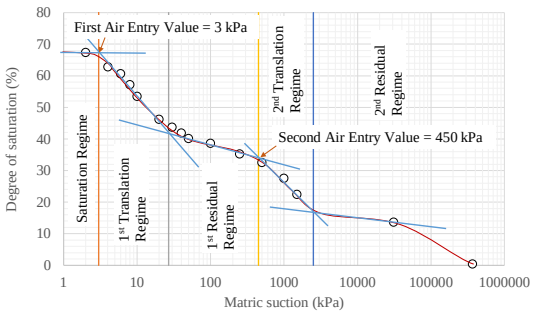

Fig. 9 Soil water characteristic curve

3.2 Consolidated drained triaxial test by multistage

The relationship between deviator stress and axial strain, as shown in Fig. 10 to 13, presented a strain softening behavior because the specimens are dense. The maximum deviator stresses as shown in Table 3 were plotted in the graph to form the Mohr-Coulomb failure envelope, as shown in Fig. 14 to 17. According to the Mohr-Coulomb (Fig. 14 to 17), it was found that the friction angle (ϕ') was not constant with a matric suction, but it was slightly increasing with matric suction as shown in Table 4. Moreover, the cohesion intercept (c) was also rising with a matric suction. The slope between the cohesion intercept (c) and matric suction, or the ϕ^b angle, is not constant, as shown in Table 3. The relationship between the cohesion intercept (c) and matric suction is non-linearly. Moreover, the ϕ^b angle is decreasing with an increase in matric suction. The graph Mohr-Coulomb failure envelope in 3D is illustrated in Fig. 18.

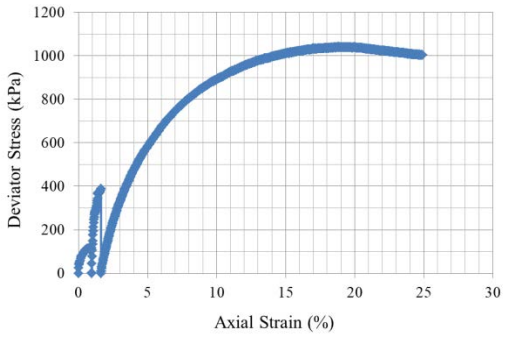

Fig. 10 The stress-strain curve derived multistage testing at matric suction of 0 kPa.

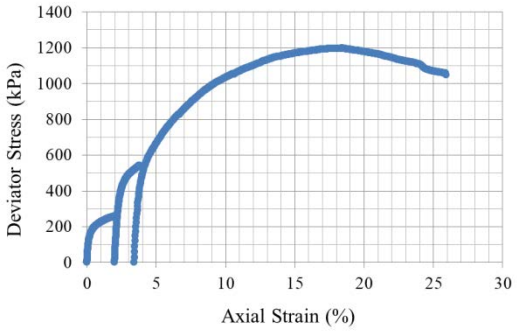

Fig. 11 The stress-strain curve derived from multistage testing at matric suction of 10 kPa.

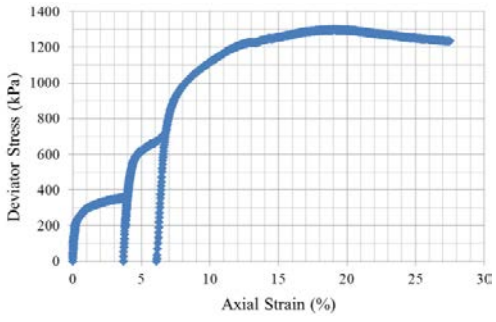

Fig. 12 The stress-strain curve derived from multistage testing at matric suction of 50 kPa.

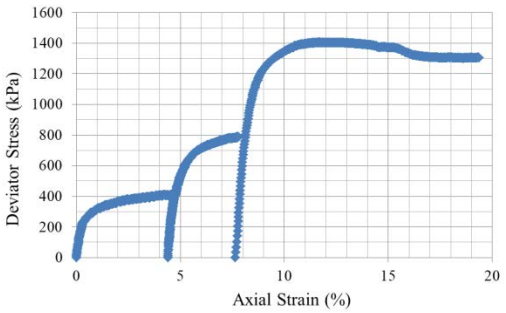

Fig. 13 The stress-strain curve derived from multistage testing at matric suction of 100 kPa.

Table 3 The maximum deviator stress

Sample No.	stage	σ_{net} (kPa)	ψ (kPa)	$\sigma_{d,max}$ (kPa)
1	1	150	0	114.6
	2	300		338.6
	3	600		1039.0
2	1	150	10	228.3
	2	300		577.0
	3	600		1125.8
3	1	150	50	358.7
	2	300		694.2
	3	600		1297.9
4	1	150	100	410.7
	2	300		787.0
	3	600		1405.0

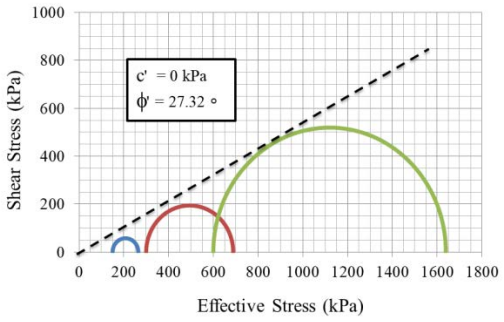

Fig. 14 Mohr-Coulomb failure envelope derived from multistage testing at matric suction of 0 kPa.

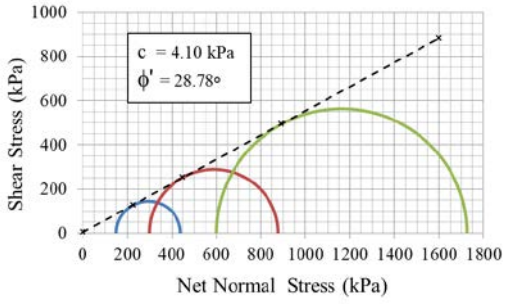

Fig. 15 Mohr-Coulomb failure envelope at matric suction of 10 kPa.

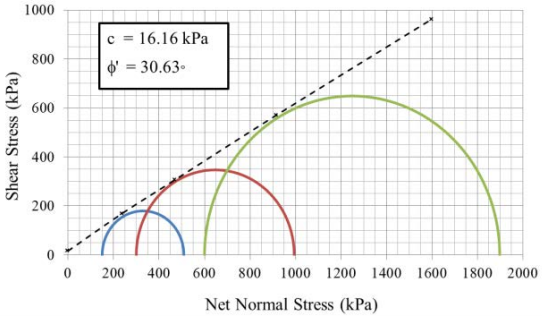

Fig. 16 Mohr-Coulomb failure envelope at matric suction of 50 kPa.

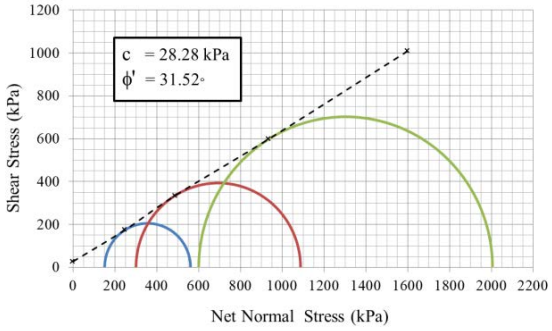

Fig. 17 Mohr-Coulomb failure envelope at matric suction of 100 kPa.

Table 4 Unsaturated shear strength parameter

Sample No.	Matric suction	Cohesion Intercept (c)	ϕ' (deg)	ϕ^b (deg)
1	0	0	27.32	27.32
2	10	4.10	28.78	22.31
3	50	16.16	30.63	16.78
4	100	28.28	31.52	13.62

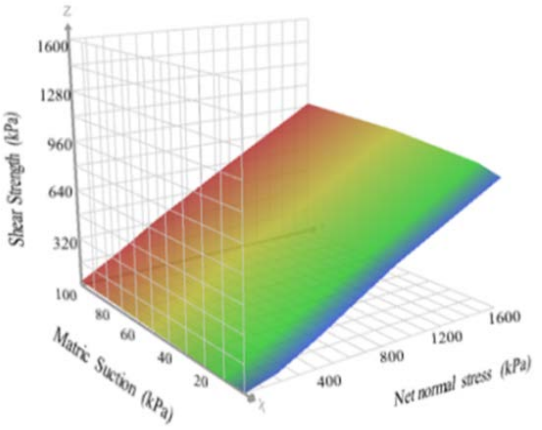

Fig. 18 The 3D graph extended the Mohr-Coulomb failure envelope.

4. DISCUSSIONS

In this part, the discussion was separated into two parts. The first part discussed the influence of matric suction on the unsaturated shear strength parameters. Then the second part was the application of the unsaturated shear strength parameter to design the earth structure.

4.1 The influence of matric suction on Khon Kaen loess

Fig. 19 presented that the shear strength was increased with a rise of the net confining pressure and matric suction. Moreover, the relationship between shear strength and matric suction was non-linear. The slope in the saturated regime is higher than the other regimes (transition and residual regime). The slope of the graph, with respect to any net confining pressure value, was not similar.

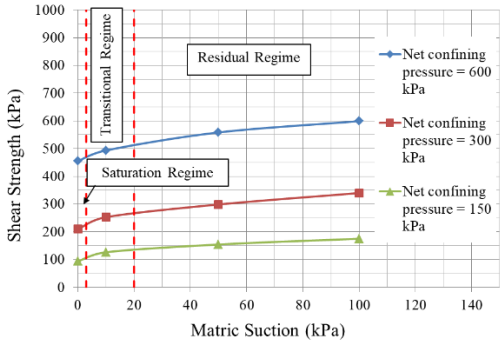

Fig. 19 The relationship between matric suction and shear strength

The relationship between matric suction and cohesion intercept (c) is quite linear as presented in Fig. 20. However, Fig. 21 showed that the value ϕ^b and ϕ' was the same value in the saturation state. Then the value of ϕ^b gradually decreased when entering the transition regime and the residual regime. Moreover, these results are consistent with the study of [10, 11, 12, and 13].

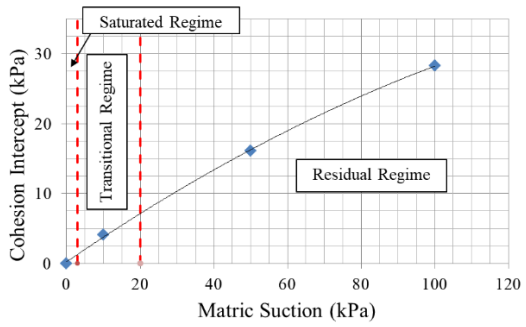

Fig. 20 The relationship between matric suction and cohesion intercept

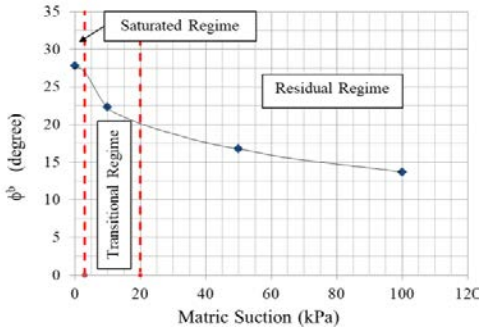

Fig. 21 The relationship between matric suction and ϕ^b

4.2 Cantilever wall design

A cantilever wall was designed from the shear strength parameters of this study. The purpose of this research was to study the influences of matric suction on the size of the cantilever wall, which consists of active earth force (P_a) and bearing capacity.

4.2.1 Active earth force (P_a)

According to the test results, the active earth forces (P_a) are as shown in Eq. (4) to (6). The active earth forces (P_a) are decreased with increasing of matric suction, as shown in Fig. 22. Therefore, the height of the retaining wall and the size of the cantilever wall can be reduced with the increase of matric suction because the earth forces acting on the walls are decreased.

$$P_A = \frac{\rho g\,(H^2 - y^2)}{N_\phi}\frac{}{2} - \frac{2c'}{\sqrt{N_\phi}}(H - y_t) - \frac{2(u_a - u_w)\tan\phi^b}{\sqrt{N_\phi}}(H - y_t) \quad (4)$$

Which;

$$y_t = \frac{2c'}{\rho g}\sqrt{N_\phi} + 2\frac{(u_a - u_w)\tan\phi^b}{\rho g}\sqrt{N_\phi} \quad (5)$$

$$N_\phi = \frac{(1+\sin\phi')}{(1-\sin\phi')} = \tan^2(45 + \frac{\phi'}{2}) \quad (6)$$

Where;

$\rho g = \gamma$ = Density of soil
H = Height of retaining wall
c' = effective apparent cohesion
u_w = pore water pressure
$_a$ = pore air pressure
$(u_a - u_w)$ = matric suction
ϕ' = friction angle of effective stress
ϕ^b = angle indicating the rate of increase in shear strength relative to the soil suction at failure plane

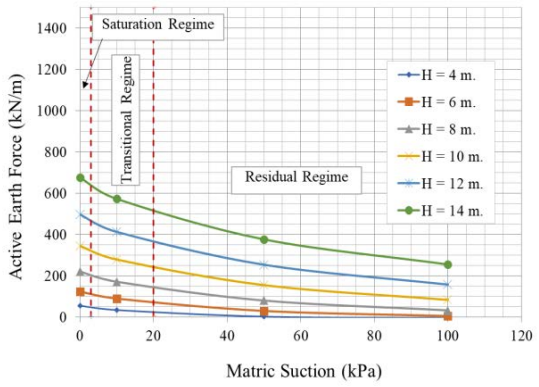

Fig. 22 Active earth force (P_a) when matric suction is constant with several heights (H).

4.2.2 Bearing capacity

The calculation of ultimate bearing capacity by using the bearing capacity equation for a strip foundation from [7] found that the ultimate bearing capacity is increased with an increase of matric suction. Therefore, the width of the cantilever wall (B) can be reduced with a rise in a matric suction value as shown in Fig. 22 due to the increase of bearing capacity of the soil.

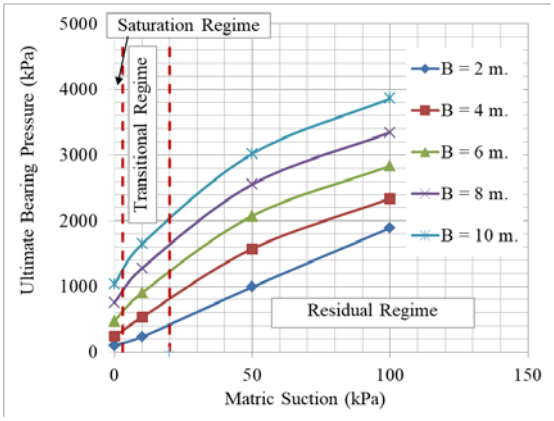

Fig. 23 Ultimate bearing capacity when matric suction is constant with several widths (B).

5. CONCLUSIONS

This research found that the drained shear strength of compacted Khon Kaen loess is increased non-linearly with an increase in matric suction. Moreover, the slope of the relationship between shear strength (τ_f) and matric suction with respect to any net confining pressure value is not similar. The effective friction angle (ϕ') is not constant with respect to matric suction. Both the effective friction angle (ϕ') and the cohesion intercepts (c) are increased with an increased matric suction. Moreover, the value ϕ^b and ϕ' were the same value in the saturation state. Then the value of ϕ^b gradually decreased when entering the transition regime and the residual regime. Therefore, this research concluded that matric suction has a significant influence on the shear strength of compacted Khon Kaen loess. Furthermore, the size of the earth structure can be optimized to save cost by using the unsaturated shear strength parameter.

6. ACKNOWLEDGMENTS

Acknowledgment is given to the SIRDC - Sustainable Infrastructure Research and Development Center, Khon Kaen University, for the support of this research.

7. REFERENCES

[1] Udomchoke V. (1991). Origin and Engineering Characteristics of the Problem Soil in the Khorat Basin, Northeastern Thailand. Ph.D. dissertation Asian Institute of Technology, Bangkok Thailand.

[2] American Society for Testing and Materials. (D2487-98). Standard practice for classification of soils for engineering purposes (Unified Soil Classification System).

[3] Chansom, D. Hormdee, T. Prachumchit, P. Weeratutsil. (2010). *A study of soil profile and settlement problems of buildings in Khon Kaen University Area.* Khon Kaen University.

[4] Gasaluck W. (1999). Influence of moisture content on bearing capacity of Khon Kaen loess. The 5th national convention on civil engineering, Pataya, Thailand.

[5] Hormdee D., Kaikeerati N., and Angsuwotai P. "Evaluation on the Results of Multistage Shear Test", Int. J. of GEOMATE, 2012, pp. 140-143 Behaviour of Concrete Containing Waste Carpet Fiber, International Journal of GEOMATE, Vol. 9, Issue 17, 2015, pp. 1441-1446.

[6] Chatchawan S., Nuntasarn R., & Hormdee D. "The comparison of drained shear strength between single stage and multistage method", 4th Int. Conf. on Science, Engineering & Environment (SEE), Nagoya, Japan, Nov.12-14, 2018, pp. 240-245.

[7] Terzaghi, K., Peck, R. B., & Mesri, G. (1996). *Soil mechanics in engineering practice*. John Wiley & Sons.

[8] Fredlund, D.G. & Rahadjo, H. (1993). Soil mechanics for unsaturated soils. New York: Wiley.

[9] Elkady, Y.T. 2002. Static and Dynamic Behaviour of Collapsible Soils. Ph.D. dissertation. The University of Arizona.

[10] Lu, N. and Likos, W.J. 2004, Filter Paper Technique for measuring total suction.

Transportation Research Record: Journal of Transportation Research Board. No. 1786, TRB, Washington, D.C., pp. 120-128.

[11] Thu, T.M., Rahardjo, H. and Leong, E.C. 2006. Shear Strength and Pore Water Pressure Characteristics during Constant Water content Triaxial Tests. Journal of Geotechnical and Geoenvironmental Engineering, vol.132, no.3, pp.411- 419.

[12] Rahardjo, H., Heng, O. B., & Choon, L. E. (2004). Shear strength of compacted residual soil from consolidated drained and constant water content triaxial tests. Canadian Geotechnical Journal, 41(3), 421-436.

[13] Al Aqtash, U., & Bandini, P. (2015). Prediction of unsaturated shear strength of an adobe soil from the soil–water characteristic curve. Construction and Building Materials, 98, 892-899.

[14] Ho, D. and Fredlund, D., "A Multistage Triaxial Test for Unsaturated Soils," Geotechnical Testing Journal, 1988, pp. 132-138.Author H., A Book New York Publisher, Year, pp.1-200.

[15] ASTM - American Society for Testing Material. Standard Test Method for Capillary-Moisture Relationships for Coarse-and Medium-Textured Soils By Porous-Plate Apparatus (ASTM D2325-98). Ann Arbor. Michigan. 1998

[16] Lu, N. and Likos. W.J., Unsaturated Soil Mechanics, Wiley, New York, 2004

[17] Gitirana Jr., Gilson de F.N. and Fredlund, D.G., Soil –Water Characteristic Curve Equation with Independent Properties, Journal of Geotechnical and Geoenvironmental Engineering, 2004, Vol. 130, No.2, pp.209-211